European Radiology
https://doi.org/10.1007/s00330-020-07618-7

MAGNETIC RESONANCE

Fetal brain tissue characterization at 1.5 T using STrategically Acquired Gradient Echo (STAGE) imaging

Feifei Qu[1] · Taotao Sun[2,3,4] · Yongsheng Chen[5] · Brijesh Kumar Yadav[1] · Ling Jiang[2,3] · Zhaoxia Qian[2,3,4] · E. Mark Haacke[1,6,7]

Received: 27 July 2020 / Revised: 13 November 2020 / Accepted: 7 December 2020

Abstract

Objectives To estimate human fetal brain MRI tissue properties including apparent T_1 (T_{1app}) and apparent proton density (PD_{app}) by using a rapid multi-contrast acquisition protocol called STrategically Acquired Gradient Echo (STAGE) imaging.

Methods STAGE data were collected using two flip angles (15° and 60°, with a TR = 600 ms) for 30 pregnant women at 1.5 T (15 healthy controls: gestational age (GA) range 19 + 1/7 weeks to 34 + 5/7 weeks; 11 abnormal subjects with ventriculomegaly: GA range 21 + 5/7 weeks to 31 + 5/7 weeks; 4 subjects with other abnormalities). Both T_{1app} and PD_{app} maps of the fetal brain were calculated from the STAGE data. A region-of-interest-based approach was used to measure T_{1app} and PD_{app} in the subplate/intermediate zone (SP/IZ), cortical plate (CP), and cerebrospinal fluid (CSF) in the fetal brain.

Results The ratios of $T_{1appSP/IZ}/T_{1appCP}$ and $PD_{appSP/IZ}/PD_{appCP}$ were larger than unity while $T_{1appSP/IZ}/T_{1appCSF}$ and $PD_{appSP/IZ}/PD_{appCSF}$ were both less than unity.

Conclusions STAGE imaging provides a potential practical approach to estimate multi-parametric properties of the human fetal brain.

Key Points

- *STAGE is feasible in measuring fetal brain tissue properties.*
- *Water content in cortical plate and subplate/intermediate zone approaches that of cerebrospinal fluid in early gestational ages.*

Keywords Fetus · Brain · Magnetic resonance imaging

Abbreviations

CP	Cortical plate
CSF	Cerebrospinal fluid
GA	Gestational age
HASTE	Half-Fourier single shot turbo spin echo
SP/IZ	Subplate/intermediate
STAGE	Strategically acquired gradient echo
VM	Ventriculomegaly

Zhaoxia Qian and E. Mark Haacke contributed equally to this work.

Feifei Qu and Taotao Sun are co-first authors.

✉ Zhaoxia Qian
zhaoxiaqian@126.com

✉ E. Mark Haacke
nmrimaging@aol.com

[1] Department of Radiology, Wayne State University School of Medicine, Detroit, MI, USA

[2] Department of Radiology, International Peace Maternity and Child Health Hospital, School of Medicine, Shanghai Jiao Tong University, Shanghai, China

[3] Shanghai Key Laboratory of Embryo Original Diseases, Shanghai, China

[4] Shandong Medical Imaging Research Institute, Shandong University, Jinan, Shandong, China

[5] Department of Neurology, Wayne State University School of Medicine, Detroit, MI, USA

[6] Department of Biomedical Engineering, Wayne State University College of Engineering, Detroit, MI, USA

[7] SpinTech, Inc., Bingham Farms, MI, USA

Published online: 01 February 2021

Introduction

Fetal brain development is a fascinating process, one not yet fully understood. Magnetic resonance imaging (MRI)-based tissue properties such as longitudinal relaxation time (T_1) and proton density (PD) can be used as biomarkers of fetal brain maturation [1–5]. Myelination of the white matter (WM) causes a decrease in T_1 and a loss of water content over time [4, 5]. It is reported that major segments of the fetal cerebral WM can be recognized between 24 and 32 weeks of gestational age (GA) [5]. In the human brain, myelination starts as early as the second trimester of pregnancy and reaches a peak during the first year after birth [5]. MRI-based studies have shown that T_1 of the neonatal brain tissue for both WM and grey matter (GM) decrease over time with the former decreasing much faster than the latter [4–6]. These findings showed that T_1 mapping could be a viable tool for monitoring the human brain maturation process. However, there are few studies reporting quantitative T_1 values for fetal brain tissue. Almajeed et al reported T_1 of the entire fetal brain with no differentiation between WM and GM at 1.5 T [7]. PD measured in MRI indicates the water content in the tissue [8]. Therefore, both T_1 and PD can be used as indicators for fetal brain tissue development.

There are many challenges in fetal brain MRI. Motion artifacts caused by fetal movement, maternal breathing, and the requirement of a large field of view (FOV) pose tremendous difficulties in fetal brain MRI. In addition, relatively long scan times cause discomfort to pregnant women. To address these issues, a rapid multi-contrast MRI technique with high resolution is desired. Recently, a fast, robust multi-contrast, parametric estimation technique referred to as STrategically Acquired Gradient Echo (STAGE) has been proposed to estimate tissue properties and has been validated in the adult brain [9–11]. This technique provides fifteen different pieces of information in just 5 min including eight qualitative images and seven quantitative images for whole brain coverage. These include T_1 and PD maps and enhanced T_1-weighted (T1W) [9, 10]. In this study, we extended the application of STAGE to image human fetuses and explored its feasibility to quantify the tissue properties of different fetal brain regions as a function of GA. As the WM and GM are still developing in the fetal brain, we focused on the subplate/intermediate zone (SP/IZ), cortical plate (CP), and cerebrospinal fluid (CSF).

Materials and methods

All subjects provided written informed consent to participate in this institutional review board approved prospective study.

Theory and simulations

STAGE is an approach employing two gradient recalled echo (GRE) sequences with a pair of optimal flip angles (FAs). The signal intensity in the GRE sequence with FA equal to θ is given by:

$$S(r,\theta) = PD \bullet bias(r) \bullet sin(k(r) \bullet \theta) \frac{1-E_1}{1-cos(k(r) \bullet \theta) \bullet E_1} \bullet E_2 \quad (1)$$

where *bias(r)* is the coil sensitivity factor at r, $E_1 = e^{-TR/T_1}$, $E_2 = e^{-TE/T_2^*}$, and *k(r)* is the B_1 field scale factor. For a low FA and a TR << T_1, Eq. (1) can be approximated as:

$$S(r,\theta) = PD_{eff} \bullet (k(r) \bullet \theta) / \left(1 + \frac{(k(r) \bullet \theta)^2}{\theta_E^2}\right) \quad (2)$$

where $PD_{eff} = PD \cdot bias(r) \cdot E_2$, and θ_E is the Ernst angle given by $\cos^{-1}(E_1)$[12]. By collecting images with two or more FAs, apparent PD and apparent T_1 can be derived from:

$$PD_{app} = k \bullet PD_{eff} \quad (3)$$

$$T_{1app} = T_1 \bullet k^2 \quad (4)$$

Consequently, the pristine k map can be obtained by fixing the T_1 value of a reference tissue such as WM [10]. However, since we do not know the value of T_1 for fetal brain SP/IZ, we use the ratios of the apparent T_1 (or apparent PD) values between CP and SP/IZ from small adjacent regions-of-interest (ROI) since the dependence on k then disappears.

The precision of T_1 mapping for the entire brain is affected by both the dynamic range (*DR*) of the two flip angles and the fractional signal of the point (*FS*), and its optimum value is achieved when the following function reaches a maximum value [13]:

$$DR \times FS = \left[\frac{S(\theta_2)}{\rho_0 \bullet \sin\theta_2} - \frac{S(\theta_1)}{\rho_0 \bullet \sin\theta_1}\right] \times \left[\frac{S(\theta_2) + S(\theta_1)}{2 \bullet S(\theta_E)}\right] \quad (5)$$

where θ_E is the Ernst angle. Assuming a T_1 of 1200 ms for fetal brain tissue [7], the two optimal FAs were found to be 22° and 90° (Fig. 1). For practical reasons, specifically to lower the specific absorption rate (SAR) and increase the signal-to-noise ratio (SNR), 15° and 60° were used in this study which gave a reduced precision for T_1 equal to 77% of the maximum value from the combination of 22° and 90°.

Patient population

In this study, the GA was calculated from the first day of the woman's last menstrual period (LMP). Counting from the first day of the LMP involved the assumption that ovulation

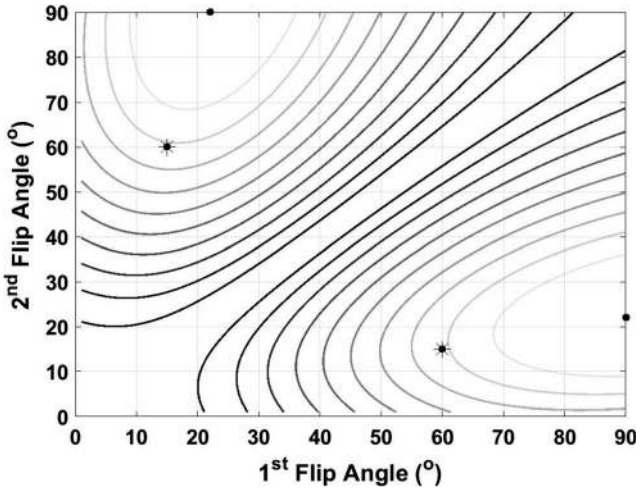

Fig. 1 Simulation of FA optimization. The contours indicate the values of the product of DR and FS. The highest value of DR × FS is indicated by the dots and occurs for FAs of 22° and 90°. The FA combination used in this work is indicated by the stars and was chosen to be 15° and 60°

occurred 14 days later. For patients receiving assisted reproductive technology whose date of ovulation was known, the 14th day before conception was used in place of the LMP. Then GA was corrected using crown rump length (CRL) [14] which was measured from an ultrasound (US) exam between 11 and 13 weeks of GA. If the difference between the corrected value and the originally recorded GA was less than 7 days, the original one was used. All subjects received a routine pregnancy examination and all babies were delivered in the hospital where the imaging took place. The clinical data at birth were recorded, and the basic neurological development status was also evaluated within 2 days after birth. The final diagnosis of which fetus would be considered normal was based on the combination of the clinical data, imaging results from MR and US, and the follow-up visit 2 months after birth.

From January 2018 to August 2018, 59 subjects were recruited in the study, among which 30 cases generated STAGE images without artifacts in the brain region at least in one slice. A total of 30 subjects with single pregnancy (15 healthy controls: GA 27.4 ± 4.8 weeks, GA range 19 + 1/7 weeks to 34 + 5/7 weeks (interquartile range 7 + 3/7 weeks (23 + 3/7 weeks, 30 + 6/7 weeks)); 11 VM cases: GA 27.2 ± 3.3 weeks; GA range 21 + 5/7 weeks to 31 + 5/7 weeks (interquartile range 4 + 5/7 weeks (24 + 3/7 weeks, 29 + 1/7 weeks)); and 4 cases with other abnormalities: GA 27.9 ± 3.8 weeks; GA range 24 + 5/7 weeks to 33 + 3/7 weeks) were used in the final data analysis.

Data acquisition

Experiments were performed on a 1.5 T Siemens Aera scanner (Siemens Healthineers) with an 8-channel body receiver coil. The subjects laid in a supine or lateral decubitus position based on their preference during the scan. The first part of the imaging protocol consisted of an initial scout sequence and a multi-slice T_2-half-Fourier single shot turbo spin echo (HASTE) sequence with the FOV covering the entire fetal brain. This was followed by the STAGE protocol using two multi-slice 2D flow-compensated single-echo GRE sequences with different FAs (15°/60°) with the following acquisition parameters: TR/TE 600 ms/18.6 ms; acquisition voxel size 0.82 × 1.64 × 3.0 mm^3; bandwidth 50 Hz/pixel; total acquisition time 1 min and 56 s for 19 slices. These two scans were repeated if motion artifacts were present in the fetal brain region. For one subject (GA 28 + 5/7 weeks, enlarged ventricle), the experiment was run with four FAs: 15°, 45°, 60°, and 70°.

Image reconstruction and data analysis

All images were processed using custom-written software in MATLAB^{TM} to obtain pixel-by-pixel T_{1app} and PD_{app} maps. For the subject scanned with four different FAs, the T_{1app} and PD_{app} maps were calculated using the four FAs and two optimal FAs (15° and 60°), respectively. A pixel-by-pixel comparison between the two groups of results was performed in the fetal brain region for a single slice.

For each of the 30 individual subjects, small ROIs inside CP, SP/IZ, and CSF were drawn manually by a radiologist with 5 years' clinical experience in fetal MR imaging from the slice best showing (SP/IZ)/CP differentiation to calculate the mean and standard deviation (SD) of T_{1app} and PD_{app}. The (SP/IZ)/CP and the (SP/IZ)/CSF regions were chosen to be adjacent to each other to reduce any slight spatial changes in the RF field variations. The analysis was carried out independently by two different observers (FQ and YC). Both inter-class (Pearson correlation coefficients (ρ)) and intra-class correlation coefficient (*ICC*) agreements were calculated. The T_2-HASTE images were used as a supplementary reference and co-registered with STAGE images to identify the brain tissue and perform ROI placement.

To limit the partial volume effect, the ROIs of CSF and SP/IZ were also checked in the two adjacent most slices to avoid covering other tissues. The CP layer is very thin; therefore, all the tissue properties were also measured from a line drawn inside the CP layer. Lin's concordance correlation (*CCC*) was calculated between the values measured in the ROIs and lines. The ratios of the tissue properties between SP/IZ and CP ($T_{1appSP/IZ}/T_{1appCP}$ and $PD_{appSP/IZ}/PD_{appCP}$), as well as SP/IZ and CSF ($T_{1appSP/IZ}/T_{1appCSF}$ and $PD_{appSP/IZ}/PD_{appCSF}$), were calculated. The errors in the T_{1app} and PD_{app} maps introduced by the image noise were estimated by using the lowest SNR in the collected images specifically in the area where CSF was evaluated (CSF has the longest T_1 and therefore the lowest signal in the T_1-weighted images). For all 30 cases collected in this study, the lowest SNR for the low FA image was 23:1, and the lowest SNR for the high FA image was 36:1.

Results

The clinical course for all subjects is listed in Table 1. It is worth noting that the diagnostic results obtained at the last ultrasound test before MRI exam from which the data in this work were collected are listed as "clinical condition by US diagnosis" in Table 1. In the final following up diagnosis, it was found that the fetus for 15 subjects have healthy fetal brain.

The pixel-by-pixel comparison between the two-FA and four-FA approaches for the T_{1app} and PD_{app} maps are plotted in Fig. 2a and b. Both methods generate comparable results (T_{1app}: ρ = 0.950, CCC 0.948; $p < 0.05$; PD_{app}: ρ = 0.982, CCC 0.977; $p < 0.05$). Bland-Altman plots are shown in Fig. 2c and d. The mean and SD bias were − 24 ± 171 ms for the T_{1app} measurements and − 2 ± 3 (arbitrary units) for the PD_{app} measurements.

Representative T_2-HASTE and T1W images, T_{1app} and PD_{app} maps for the brain of a 29 weeks fetus, as well as delineation of ROIs are shown in Fig. 3. CP, SP/IZ, and CSF can be identified clearly in all the images except the PD_{app} map. At this early stage in fetal development, the PD_{app} map shows low contrast between CP, SP/IZ, and CSF. In the T1W images, CP is brighter than SP/IZ and CSF. Excellent inter-class and intra-class agreements were found in all tissue measurements (Table 2). The *CCC* between the tissue properties measured by the ROI and line approaches were high (observer 1: T_{1app} 0.983, PD_{app} 0.992; observer 2: T_{1app} 0.931, PD_{app} 0.985). All the tissue property values in the data analysis in the work were measured using the ROI approach. The maximum error introduced by the noise in the T_{1app} estimation was 0.63% and for PD_{app} was 0.25%. The mean and SD of the T_{1app}, PD_{app} values, the ratios between SP/IZ and CP, and SP/IZ and CSF of healthy controls and VM subjects are listed in Table 3. The *t* test values (*P*) between the two groups are shown in the table. No significant difference was found in any tissue properties. The clinical course and tissue properties of the other 4 abnormal subjects are provided in the supplementary material. The T_1 value of WM in neonatal brain at 1.5 T was reported as 1712 ± 235 ms, and the T_1 value of GM was reported as 1144 ± 245 ms [15]. Both of them are very similar with the values found in this study.

The tissue properties for all 30 subjects are plotted in Fig. 4, and the ratios of the tissue properties are plotted in Fig. 5. Both Pearson correlation coefficients (ρ) and *t* test values between tissue properties and GA in healthy controls and VM subjects are given in Table 3. For most of the cases, $T_{1appCSF} > T_{1appSP/IZ} > T_{1appCP}$ and $PD_{appCSF} > PD_{appSP/IZ} > PD_{appCP}$. Figure 4 shows that $T_{1SP/IZ}$, T_{1CP}, $PD_{SP/IZ}$, and PD_{CP} varied through GA; however, there was no significant correlation found in either healthy controls group or VM group (Table 4).

Figure 5 shows the behavior of the different measures across GA. Specifically, there was no significant correlation for any of the measures: $T_{1appSP/IZ}/T_{1appCP}$ ($\rho_{control}$ = 0.1939, $p_{control}$ = 0.4899, ρ_{VM} = 0.5672, P_{VM} = 0.0688), $PD_{appSP/IZ}/PD_{appCP}$ ($\rho_{control}$ = 0.3125, $p_{control}$ = 0.2568, ρ_{VM} = 0.3292, P_{VM} = 0.3228), $T_{1appSP/IZ}/T_{1appCSF}$ ($\rho_{control}$ = − 0.1163, $p_{control}$ = 0.6797, ρ_{VM} = 0.2432, P_{VM} = 0.4711), and $PD_{appSP/IZ}/PD_{appCSF}$ ($\rho_{control}$ = − 0.3591, $p_{control}$ = 0.1887, ρ_{VM} = − 0.0343, P_{VM} = 0.9203) across GA.

Discussion

In this study, we have applied the STAGE technique to fetal brain imaging and mapping of T_1 and PD. The tissue property

Table 1 Clinical condition for all subjects

Clinical condition by US diagnosis	Enlarged ventricle	Intrauterine growth restriction (IUGR)	Enlarged posterior fossa cisterna	Biparietal diameter (BPD) smaller than GA	Arachnoid cyst	Congenital talipes equinovarus
Number of subjects	11 (10 + 1*)	2	2*	1	1	1
Number of healthy fetal brains	0	1	1	1	1	0
Clinical condition by US diagnosis	Non-echo in posterior fossa	Sacrococcygeal structure not clear	Septa lucidum not clear	Placenta increta	Previous cesarean section and low-lying placenta	Renal cyst
Number of subjects	1	1	1	1	2	1
Number of healthy fetal brains	1	1	1	1	2	1
Clinical condition by US diagnosis	Choroid fissure cysts	Renal dysplasia	Pulmonary artery widening	Enlarged kidneys	Possible gastrointestinal dysplasia	Late spontaneous abortion
Number of subjects	1	1	1	1	1	1
Number of healthy fetal brains	0	0	1	1	1	1

*This case has both an enlarged ventricle and an enlarged posterior fossa cisterna

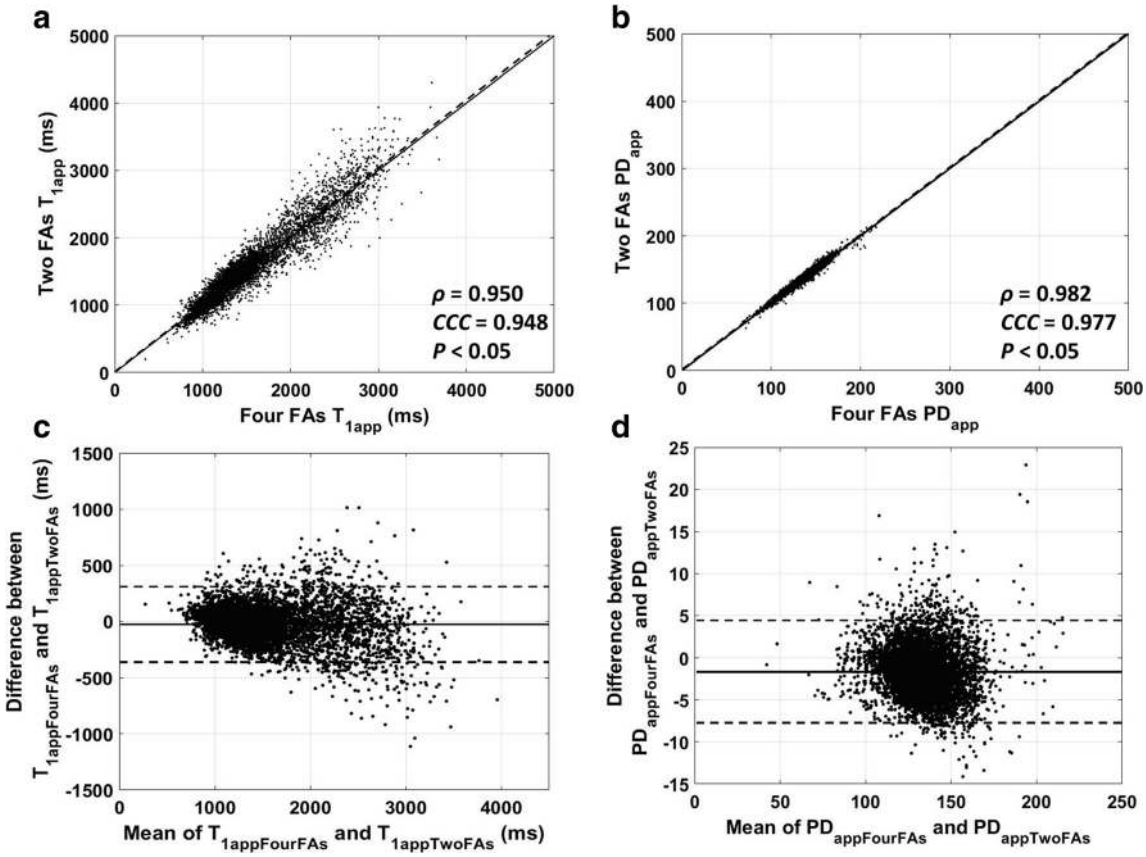

Fig. 2 Comparison between the tissue properties pixel-by-pixel. A total of 5905 pixels were used from a single slice brain region. For both (**a**) T_{1app} and (**b**) PD_{app}, the two-FA approach generated comparable results to the four-FA approach. The linear fitting of T_{1app} and PD_{app} (dashed line) almost overlay onto the lines of identity (solid line). Bland-Altman plots were performed for (**c**) T_{1app} and (**d**) PD_{app} estimation from the two-FA approach and the four-FA approach. The mean bias for T_{1app} was − 24 ms and for PD_{app} was − 2 (arbitrary units)

maps generated by the two-FA versus the four-FA STAGE approach were comparable with each other. We found that $T_{1appSP/IZ}$ is higher than T_{1appCP} in fetal brain, in agreement with fetal T_1 values reported in a previous work [7]. This is in agreement with the results of neonatal brain studies [6]. It is well known that both T_{1WM} and T_{1GM} decrease with age during the first post-natal year, which is generally associated with the process of myelination [5]. It has been shown that T_{1WM} is still longer than T_{1GM} for neonates at birth. Both of them decrease rapidly though time during the first year, and T_{1WM} decreases much faster than T_{1GM}. T_{1WM} becomes shorter than T_{1GM} within roughly 6 months. T_{1WM} decreases to adult relaxation values at about 2 years, and T_{1GM} decreases to adult relaxation values at about 1.5 years [6]. However, in our study, no trend for $T_{1SP/IZ}/T_{1CP}$ was found.

The T_1 of brain tissues change with the myelination process, as does the water content (effectively the PD) [1–5, 8]. Therefore, these two parameters could be used as tools to

Table 2 Inter-rater and intra-class correlation results from the two observers

Tissue	Tissue property	ICC	Pearson correlation coefficient (ρ)
SP/IZ (close to CSF)	T_{1app}	0.933 ($p < 10^{-10}$)	0.946
	PD_{app}	0.988 ($p = 0$)	0.991
SP/IZ (close to GM)	T_{1app}	0.943 ($p < 10^{-10}$)	0.945
	PD_{app}	0.991 ($p = 0$)	0.991
CP (ROI)	T_{1app}	0.946 ($p < 10^{-10}$)	0.949
	PD_{app}	0.993 ($p = 0$)	0.994
CP (line)	T_{1app}	0.928 ($p < 10^{-10}$)	0.947
	PD_{app}	0.985 ($p = 0$)	0.985
CSF	T_{1app}	0.963 ($p < 10^{-10}$)	0.964
	PD_{app}	0.997 ($p = 0$)	0.997

Table 3 T_{1app} and PD_{app} values of brain tissues in healthy controls and VM subjects

Tissue	Controls	Tissue properties				VM cases	Tissue properties				*t* test (*p* value)	Tissue properties	
		T_{1app} (ms)		PD_{app}			T_{1app} (ms)		PD_{app}			T_{1app}	PD_{app}
		Mean	Std	Mean	Std		Mean	Std	Mean	Std			
SP/IZ		1498	279	242	67		1639	237	271	85		0.1873	0.3483
CP		1235	307	230	66		1283	270	255	84		0.6804	0.4056
CSF		2655	432	272	81		2755	500	307	97		0.5884	0.3300
		Relative Tissue Properties					Relative Tissue Properties					Relative Tissue Properties	
		T_{1app} Ratio		PD_{app} Ratio			T_{1app} Ratio		PD_{app} Ratio			T_{1app} Ratio	PD_{app} Ratio
		Mean	Std	Mean	Std		Mean	Std	Mean	Std			
(SP/IZ)/CP		1.24	0.15	1.06	0.05		1.30	0.17	1.07	0.06		0.3248	0.5529
(SP/IZ)/CSF		0.5930	0.0664	0.9401	0.0358		0.6034	0.0500	0.9333	0.0566		0.6664	0.7077

monitor brain development and investigate the tissue change during the maturation process and to probe pathophysiological changes. A few studies have reported brain tissue T_1 variation during development in neonatal subjects and showed that T_1 of GM and WM decrease with different rates over time [4, 6]. However, few studies have focused on the tissue properties of fetal brain [7]. The reason for this is because of the challenges in fetal brain MR imaging, including motion issues, the requirement of a large FOV with high resolution and potentially high SAR. Therefore, a fast, high resolution, low SAR mapping technique is required for fetal tissue characterization. Although the STAGE acquisition takes roughly 2 min to cover the entire fetal brain which is a long time given that the fetus can move during the scan, STAGE has the advantage that it offers multiple contrasts and multiple quantitative tissue property maps [11]. In our previous work, we reported the use of susceptibility-weighted imaging and quantitative susceptibility mapping (QSM) in the human fetuses with enlarged brain ventricles by using STAGE [16]. These two sets of images can be related to tissue oxygenation. Combining the PD and T_1 maps with QSM and R_2* maps makes STAGE an attractive means to study fetal brain and fetal brain development. In practice, the TR could be reduced to 30 ms so that its scan would take only several seconds per slice, but there would be a major loss of signal-to-noise that would compromise the value of these images. Nevertheless, with the use of 3 T imaging and better designed surface coils for fetal imaging to improve SNR, this rapid single slice approach could become viable in the future.

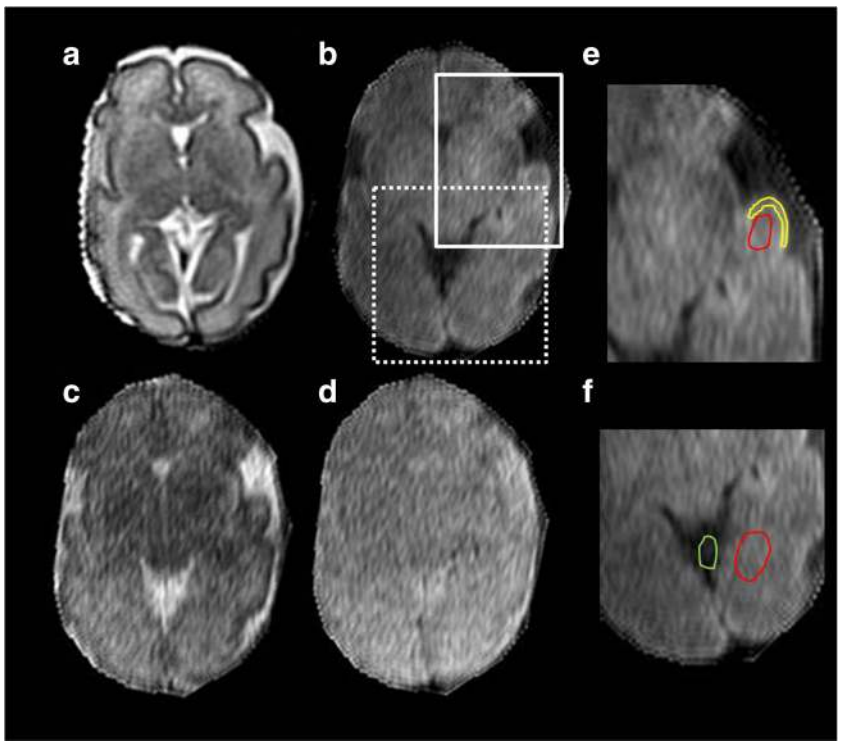

Fig. 3 T_1-weighted images and tissue property maps from a fetus of 29 weeks gestational age. **a** T_2-HASTE image. **b** T1W image. **c** T_{1app} map. **d** PD_{app} map. The highlighted boxes in **b** are zoomed in (**e**) and (**f**). The regions-of-interest of SP/IZ are marked in red, of CP in yellow, and of CSF in green

Table 4 Statistical results for tissue properties versus GA in healthy controls and VM subjects

Controls				
	$T_{1appSP/IZ}$ vs. GA	T_{1appCP} vs. GA	$T_{1appSP/IZ}/T_{1appCP}$ vs. GA	$T_{1appSP/IZ}/T_{1appCSF}$ vs. GA
Pearson correlation coefficient (ρ)	− 0.300	− 0.1561	0.1939	− 0.1163
t test value (p)	0.9154	0.5786	0.4899	0.6797
	$PD_{appSP/IZ}$ vs. GA	PD_{appCP} vs. GA	$PD_{appSP/IZ}/PD_{appCP}$ vs.GA	$PD_{appSP/IZ}/PD_{appCSF}$ vs. GA
Pearson correlation coefficient (ρ)	− 0.1208	− 0.1778	0.3125	− 0.3591
t test value (p)	0.6680	0.526	0.2568	0.1887
VM cases				
	$T_{1appSP/IZ}$ vs. GA	T_{1appCP} vs. GA	$T_{1appSP/IZ}/T_{1appCP}$ vs. GA	$T_{1appSP/IZ}/T_{1appCSF}$ vs. GA
Pearson correlation coefficient (ρ)	− 0.2799	− 0.5655	0.5672	0.2432
t test value (p)	0.4045	0.0698	0.0688	0.4711
	$PD_{appSP/IZ}$ vs. GA	PD_{appCP} vs. GA	$PD_{appSP/IZ}/PD_{appCP}$ vs.GA	$PD_{appSP/IZ}/PD_{appCSF}$ vs. GA
Pearson correlation coefficient (ρ)	− 0.2567	− 0.2943	0.3292	− 0.0343
t test value (p)	0.4460	0.3796	0.3328	0.9203

One of the difficulties in the current study is that we do not have accurate radiofrequency (RF) transmitter and receiver field correction. Therefore, instead of obtaining actual tissue T_1 and PD values, T_{1app} and PD_{app} (which include the effects of RF penetration) were used. To reduce the RF penetration effect, the SP/IZ ROIs were placed adjacent to either CSF or CP so that a ratio of values insensitive to RF penetration could be obtained (since all local tissues have the same dependence on the RF transmit field correction) [10]. In this study, no motion correction was performed, rather instead, we repeated the data acqusition once for those scans with severe motion artifiacts. To evaluate the fetal brain shift between two scans, an intersection over union (IoU) for the entire brain region was calculated from the same slice used in the STAGE imaging analysis. The average IoU for the 30 subjects was 0.94 with an SD of 0.04 indicating there was a minor displacement of the fetal brain between the two images.

There are several limitations to this study. First, more controls and VM cases are required to investigate the brain tissue property differences between the two groups as well as changes across GA. One cause of enlarged ventricles in the fetal brain is the disturbance to myelinogenesis [17]. Despite this, we did not find significant differences between the control and VM groups in any fetal brain tissue properties. More subjects are needed to draw a solid conclusion. Second, the acquisition resolution may not be high enough to avoid partial volume effects in the thin CP layer. Third, there is a small remnant T_2^* effect left in the PD_{app} estimation. In this study, only a single-echo sequence was used and tissue T_2^* could not be estimated. Finally, RF receive and transmit coil effects were not globally

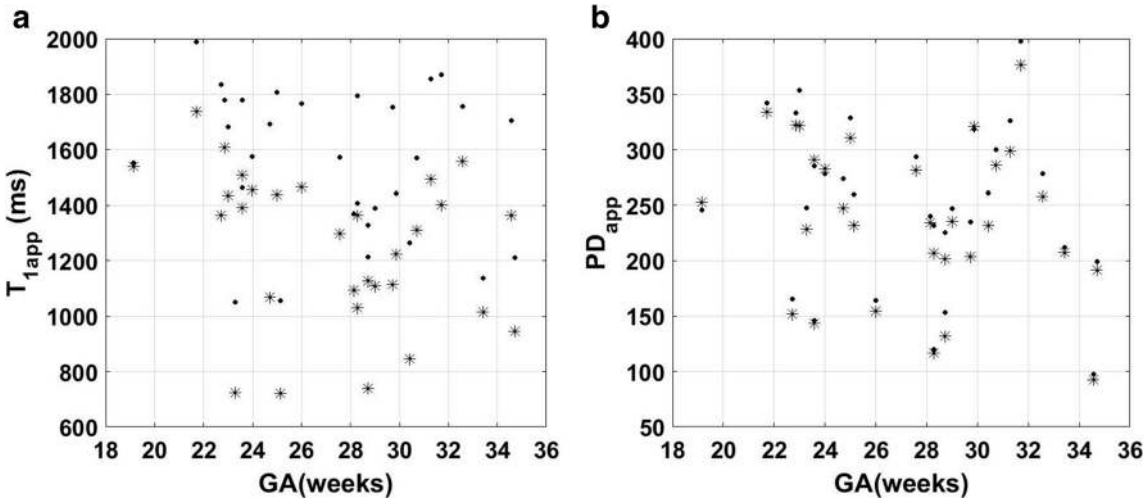

Fig. 4 T_{1app} and PD_{app} values of SP/IZ (dots) and CP (asterisks) for all subjects. **a** T_{1app} values of SP/IZ and CP for all subjects. **b** PD_{app} values of SP/IZ and CP for all subjects. The controls are marked by circles, and the VM cases are marked by triangles. The four unmarked points are the abnormal subjects with other clinical conditions. These values have not been corrected for radiofrequency field variations

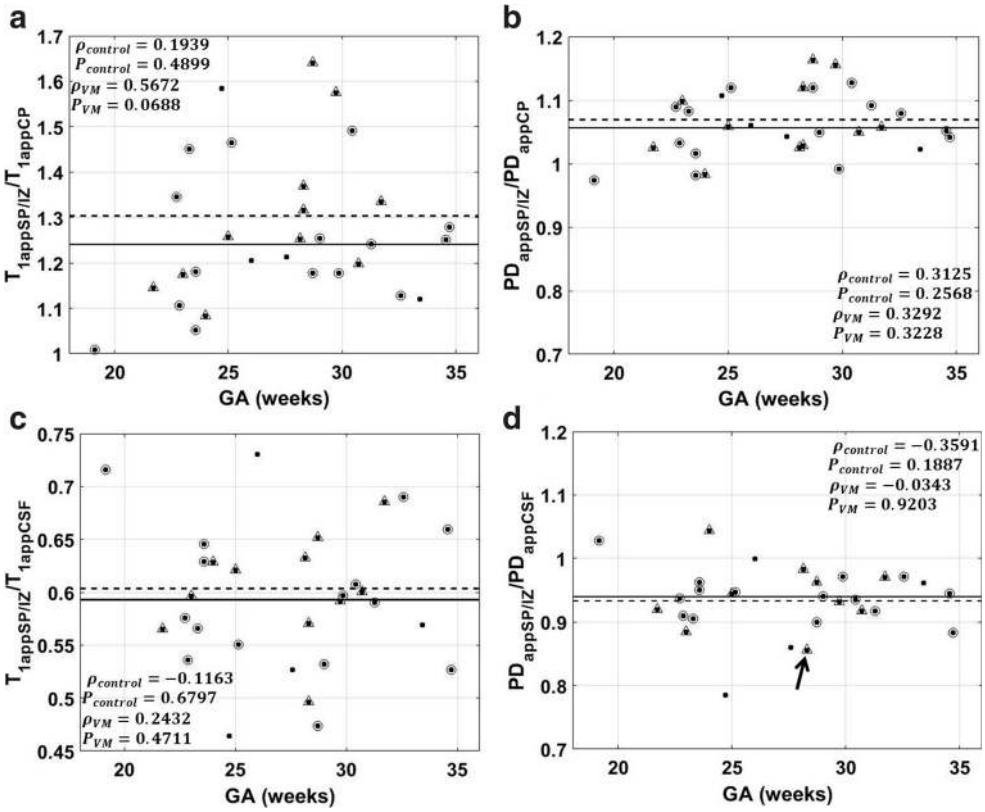

Fig. 5 T_{1app} and PD_{app} ratios between different brain tissues for all subjects. **a** $T_{1appSP/IZ}/T_{1appCP}$ values for all subjects. **b** $PD_{appSP/IZ}/PD_{appCP}$ values for all subjects. **c** $T_{1appSP/IZ}/T_{1appCSF}$ values for all subjects. **d** $PD_{appSP/IZ}/PD_{appCSF}$ values for all subjects. The dots show the tissue property for each subject. The solid lines show the mean values of the controls, and the dashed lines show the mean values of the VM cases. All the controls are marked by circles, and the VM cases are marked by triangles. The four unmarked points are the abnormal subjects with other clinical conditions. There appears to be only 29 data points because two overlap; these two points that overlapped are indicated by the arrow

addressed. In the future, broader measurements would be possible throughout all tissues without the need for ratios could then be collected to improve the statistics.

In conclusion, in this feasibility study, we have implemented the STAGE imaging protocol in both healthy controls and VM subjects to estimate T_{1app} and PD_{app} for fetal brain tissues. The most significant findings were $T_{1appSP/IZ}/T_{1appCP}$ and $PD_{appSP/IZ}/PD_{appCP}$ were greater than unity as expected in fetal SP/IZ.

Supplementary Information The online version contains supplementary material available at https://doi.org/10.1007/s00330-020-07618-7.

Funding The authors state that this work has not received any funding.

Compliance with ethical standards

Guarantor The scientific guarantor of this publication is Dr. E. Mark Haacke.

Conflict of interest E. M. Haacke is the Chief Scientific Officer of SpinTech.

Statistics and biometry One of the authors has significant statistical expertise.

Informed consent Written informed consent was obtained from all subjects (patients) in this study.

Ethical approval Institutional Review Board approval was obtained.

Methodology
- prospective
- experimental

References

1. Girard N, Raybaud C, Poncet M (1995) In vivo MR study of brain maturation in normal fetuses. AJNR Am J Neuroradiol 16:407–413
2. Wang Z, Chen J, Qin Z, Zhang J (1998) The research of myelinization of normal fetal brain with magnetic resonance imaging. Chin Med J (Engl) 111:71–74
3. Garel C, Chantrel E, Elmaleh M, Brisse H, Sebag G (2003) Fetal MRI: normal gestational landmarks for cerebral biometry, gyration and myelination. Childs Nerv Syst 19:422–425
4. Barkovich AJ (2000) Concepts of myelin and myelination in neuroradiology. AJNR Am J Neuroradiol 21:1099–1109
5. Dubois J, Dehaene-Lambertz G, Kulikova S, Poupon C, Huppi PS, Hertz-Pannier L (2014) The early development of brain white matter: a review of imaging studies in fetuses, newborns and infants. Neuroscience 276:48–71
6. Holland BA, Hass DK, Norman D, Brant-Zawadzki M, Newton TH (1986) MRI of normal brain maturation. AJNR Am J Neuroradiol 7:201–208
7. Almajeed AA, Adamsbaum C, Langevin F (2004) Myelin characterization of fetal brain with mono-point estimated T1-maps. Magn Reson Imaging 22:565–572
8. Cercignani M, Dowell NG, Tofts P (2018) Quantitative MRI of the brain: principles of physical measurement, 2nd edn. CRC Press Taylor & Francis Group, Boca Raton

9. Chen YS, Liu SF, Wang Y, Kang Y, Haacke EM (2018) STrategically Acquired Gradient Echo (STAGE) imaging, part I: creating enhanced T1 contrast and standardized susceptibility weighted imaging and quantitative susceptibility mapping. Magn Reson Imaging 46:130–139
10. Wang Y, Chen YS, Wu DM et al (2018) STrategically Acquired Gradient Echo (STAGE) imaging, part II: correcting for RF inhomogeneities in estimating T1 and proton density. Magn Reson Imaging 46:140–150
11. Haacke EM, Chen YS, Utriainen D et al (2020) STrategically Acquired Gradient Echo (STAGE) imaging, part III: technical advances and clinical applications of a rapid multi-contrast multi-parametric brain imaging method. Magn Reson Imaging 65:15–26
12. Haacke EM, Brwon RW, Thompson MR, Venkatesan R (1999) Magnetic resonance imaging: physical principles and sequence design, 1st edn. Wiley-Liss, New York
13. Deoni SC, Rutt BK, Peters TM (2003) Rapid combined T1 and T2 mapping using gradient recalled acquisition in the steady state. Magn Reson Med 49:515–526
14. Loughna P, Chitty L, Evans T, Chundleigh Y (2009) Fetal size and dating: charts recommended for clinical obstetric practice. Ultrasound 17:160–166
15. Jones RA, Palasis S, Grattan-Smith JD (2004) MRI of the neonatal brain: optimization of spin-echo parameters. AJR Am J Roentgenol 182:367–372
16. Yadav BK, Sun TT, Qu FF, Haacke EM, Jiang L, Qian ZX (2019) Cerebral venous oxygenation in the human fetuses with enlarged-ventricles using QSM. In: Proceedings of the Joint Annual Meeting ISMRM-ESMRMB. Montreal, Canada 1643
17. Leviton A, Gilles F (1996) Ventriculomegaly, delayed myelination, white matter hypoplasia, and "periventricular" leukomalacia: how are they related? Pediatr Neurol 15:127–136